

1,1'-Ferrocenedicarboxylate-Bridged Redox-Active Organotin and -tellurium-Containing 16-Membered Macrocycles: Synthesis, Structure, and Electrochemistry

Vadapalli Chandrasekhar* and Ramalingam Thirumoorthi

Department of Chemistry, Indian Institute of Technology Kanpur, Kanpur 208016, India

Received June 22, 2007

The reaction of 1,1'-ferrocenedicarboxylic acid, LH₂, with diorganotin halides R₂SnCl₂ (R = *n*-Bu and Bn) or Ar₂TeCl₂ (Ar = 4-OMe-C₆H₄) in the presence of triethylamine afforded, in nearly quantitative yields, heterobimetallic tetranuclear macrocycles [R₂SnL]₂ and [Ar₂TeL]₂. The molecular structures of these compounds have been confirmed by single-crystal X-ray analysis and show that the two main-group metal atoms within each macrocycle are bridged to each other by two ferrocene carboxylate ligands. In the case of the organotin derivatives the ferrocenedicarboxylate ligand acts in an anisobidentate chelating manner, leading to a hexacoordinate tin present in a skewed trapezoidal bipyramid geometry. In contrast, in the tellurium analogue the ferrocenecarboxylate ligand is monodentate, leading to a tetracoordinate tellurium in a *seesaw* geometry. ESI-MS studies on these macrocyclic complexes reveal that they retain their structural integrity in solution. Electrochemical studies reveal that [n-Bu₂SnL]₂ and [Ar₂TeL]₂ show two quasi-reversible oxidation processes. These compounds have low comproportionation constants (K_c) and can be described as being intermediate between noncoupling and weakly coupled systems. [Bn₂-SnL]₂ also shows two oxidation processes. However, in this instance, the second event is irreversible.

Introduction

Recently there has been considerable interest in the application of inorganic rings and cages as scaffolds for the preparation of multiredox compounds.¹ We have shown the successful utilization of cyclophosphazenes and Sn–O-containing compounds for the preparation of multiferrocene assemblies.² Organostannoxane-supported multiferrocene assemblies are readily prepared in a reaction involving an organotin precursor and ferrocenecarboxylic acid. The main advantages of this protocol are (a) one-pot single-step synthesis and excellent yields, (b) modulation of the number of ferrocene units by stoichiometric control as well as by the choice of organotin precursor, and (c) redox stability of the multiferrocene assemblies. We were interested in determining if the above methodology can be extended to 1,1'-ferrocenedicarboxylic acid, LH₂ (**1**). We were aware that in general the reactions of dicarboxylic acids with organotin precursors afford insoluble coordination polymers.³ However, recently we and others have shown the isolation and characterization of tractable products

in some of these reactions.⁴ Prior to the current work, Ma and co-workers have investigated the reactions of **1** with *n*-Bu₂SnO under solvothermal conditions, in an autoclave at 180 °C, and isolated a completely dealkylated octanuclear cage [Sn₈O₄L₆].⁵ This compound was not electrochemically stable and decomposed under cyclic voltammetric conditions. In another report utilization of **1** to replace a bridging carbonate ligand in a double-ladder organotin cluster was reported.⁶ Electrochemical behavior of the latter was not reported. Recently two other reports on the reactions of diorganotin compounds with **1** have appeared, although in neither case has an X-ray crystal structure or electrochemical behavior been reported.⁷ In the following, we report the synthesis, structural characterization, and electrochemistry of organotin macrocycles containing ferrocenedicarboxylate ligands, [R₂SnL]₂ [R = *n*-Bu (**2**), Bn (**3**)]. For comparing the applicability of the above synthetic procedure, we also prepared and characterized a diorganotellurium analogue [Ar₂TeL]₂ [Ar = 4-OMe-C₆H₄ (**4**)]. Unlike organotin compounds, organotellurium compounds containing ferrocenecarboxylate ligands are unknown. The macrocycle **4** represents the first example of a structurally characterized organotellurium

* To whom correspondence should be addressed. E-mail: vc@iitk.ac.in. Phone: (+91) 512-259-7259. Fax: (+91) 512-259-0007/7436.

(1) (a) Baskar, V.; Roesky, P. W. *Dalton Trans.* **2006**, 676. (b) MacLachlan, M. J.; Zheng, J.; Lough, A. J.; Manners, I. *Organometallics* **1999**, *18*, 1337. (c) Prokopuk, N.; Shriver, D. F. *Inorg. Chem.* **1997**, *36*, 5609. (d) Kondo, M.; Shinagawa, R.; Miyazawa, M.; Kabir, M. K.; Irie, Y.; Horiba, T.; Naito, T.; Maeda, K.; Utsuno, S.; Uchida, F. *Dalton Trans.* **2003**, 515. (e) Kumar, S. S.; Reddy, N. D.; Roesky, H. W.; Vidovic, D.; Magull, J.; Winter, R. F. *Organometallics* **2003**, *22*, 3348. (f) Uhl, W.; Spies, T.; Haase, D.; Winter, R.; Kaim, W. *Organometallics* **2000**, *19*, 1128. (g) Das, N.; Arif, A. M.; Stang, P. J. *Inorg. Chem.* **2005**, *44*, 5798.

(2) (a) Chandrasekhar, V.; Nagendran, S.; Bansal, S.; Kozee, M. A.; Powell, D. R. *Angew. Chem. Int. Ed.* **2000**, *39*, 1833. (b) Chandrasekhar, V.; Gopal, K.; Nagendran, S.; Singh, P.; Steiner, A.; Zacchini, S.; Bickley, J. F. *Chem.—Eur. J.* **2005**, *11*, 5437. (c) Chandrasekhar, V.; Nagendran, S.; Bansal, S.; Cordes, A. W.; Vijji, A. *Organometallics* **2002**, *21*, 3297. (d) Chandrasekhar, V.; Andavan, G. T. S.; Nagendran, S.; Krishnan, V.; Azhakar, R.; Butcher, R. J. *Organometallics* **2003**, *22*, 976.

(3) (a) Andrews, T. M.; Bower, F. A.; LaLiberte, B. R.; Montermoso, J. C. *J. Am. Chem. Soc.* **1958**, *80*, 4102. (b) Gielen, M.; Melotte, M.; Atassi, G.; Willem, R. *Tetrahedron* **1989**, *45*, 1219.

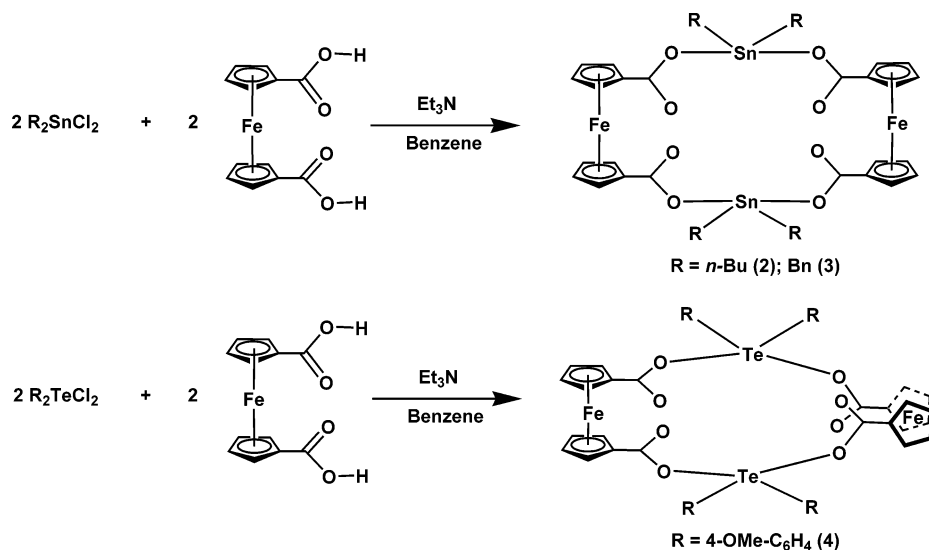
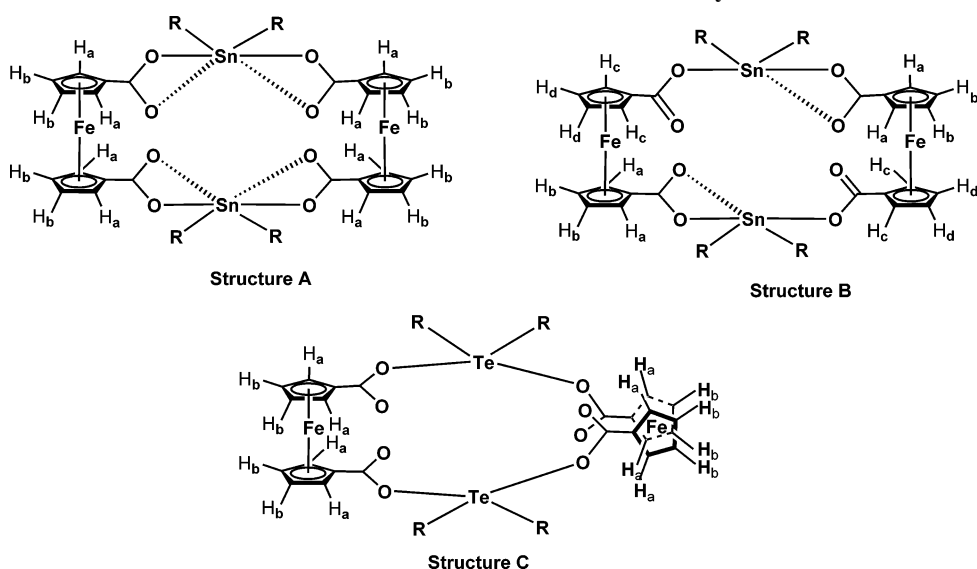
(4) (a) Chandrasekhar, V.; Thirumoorthi, R.; Azhakar, R. *Organometallics* **2007**, *26*, 26. (b) Garcia-Zarracino, R.; Höpfl, H. *J. Am. Chem. Soc.* **2005**, *127*, 3120. (c) Garcia-Zarracino, R.; Ramos-Quiñones, J.; Höpfl, H. *Inorg. Chem.* **2003**, *42*, 3835. (d) Garcia-Zarracino, R.; Höpfl, H. *Angew. Chem., Int. Ed.* **2004**, *43*, 1507. (e) Nicola, C. D.; Galindo, A.; Hanna, J. V.; Marchetti, F.; Pettinari, C.; Pettinari, R.; Rivarola, E.; Skelton, B. W.; White, A. H. *Inorg. Chem.* **2005**, *44*, 3094. (f) Ma, C.; Sun, J. *Dalton Trans.* **2004**, 1785. (g) Wengrovius, J. H.; Garbuzkas, M. F. *Organometallics* **1992**, *11*, 1334.

(5) Zheng, G.-L.; Ma, J.-F.; Su, Z.-M.; Yan, L.-K.; Yang, J.; Li, Y.-Y.; Liu, J.-F. *Angew. Chem., Int. Ed.* **2004**, *43*, 2409.

(6) Zheng, G.-L.; Ma, J.-F.; Yang, J.; Li, Y.-Y.; Hao, X.-R. *Chem.—Eur. J.* **2004**, *10*, 3761.

(7) (a) Carraher, C. E.; Morie, K. *J. Inorg. Organomet. Polym. Mater.* **2007**, *17*, 127. (b) Tao, J.; Xiao, W. *J. Organomet. Chem.* **1996**, *526*, 21.

Scheme 1. Synthesis of Compounds 2–4

Chart 1. Structures of the Heterobimetallic Macrocycles 2–4^a

^a The number of chemically equivalent cyclopentadienyl protons for each structure is indicated.

compound containing ferrocene ligands. Further, although a number of organotin cages and clusters are known,⁸ the number of authentic examples of organotin-containing macrocycles are still relatively quite few,^{9a–c} particularly those that retain their solid-state structures in solution.^{4b,9d}

Results and Discussion

Synthesis. As mentioned above, the solvothermal reaction of ferrocenedicarboxylic acid, LH₂ (**1**), with *n*-Bu₂SnO has been reported to afford a completely dealkylated mixed-valent octanuclear cage [Sn₈O₄L₆].⁵ In contrast, we have found that

the reaction of **1** with *n*-Bu₂SnCl₂, Bn₂SnCl₂, and Ar₂TeCl₂ (Ar = 4-OMe-C₆H₄) in the presence of triethylamine proceeds smoothly to afford, in near quantitative yields, 16-membered heterobimetallic tetranuclear (Sn₂Fe₂ and Te₂Fe₂) macrocycles, [R₂SnL]₂ [R = *n*-Bu (**2**); R = Bn (**3**)] and [Ar₂TeL]₂ (**4**) (Scheme 1). Compounds **2–4** show parent ion [M + H]⁺ peaks in their ESI-MS spectra indicating the structural integrity of the macrocycles under these conditions (Figures S1–S4). It may also be noted that under the ESI-MS conditions high-intensity peaks are observed for the symmetrically fragmented species: [*n*-Bu₂SnL + H]⁺ (**2**) at *m/z* = 507.02; [Bn₂SnL + H]⁺ (**3**) at *m/z* = 575.00; and [Ar₂TeL + H]⁺ (**4**) at *m/z* = 616.99. The ¹¹⁹Sn NMR spectra of **2** and **3** are singlets and resonate at –152.2 and –259.2 ppm, respectively. The chemical shift of **2** is comparable to that found in the mononuclear compound *n*-Bu₂Sn[FcCO₂]₂ (–158.6 ppm).^{2b} The chemical shift of **3** is comparable to that found for dibenzyltin(IV) dibenzoate (–252.5 ppm).^{9f} Examination of the ¹¹⁹Sn chemical shifts reveals that the chemical shift observed for **2** corresponds to a five-coordinate tin.^{4g} The X-ray crystal structure analysis of **2** reveals a six-coordinate tin due to anisobidentate chelation of two

(8) (a) Chandrasekhar, V.; Gopal, K.; Thilagar, P. *Acc. Chem. Res.* **2007**, *40*, 420. (b) Chandrasekhar, V.; Nagendran, S.; Baskar, V. *Coord. Chem. Rev.* **2002**, *235*, 1. (c) Chandrasekhar, V.; Gopal, K.; Sasikumar, P.; Thirumoorthi, R. *Coord. Chem. Rev.* **2005**, *249*, 1745.

(9) (a) Prabusankar, G.; Murugavel, R. *Organometallics* **2004**, *23*, 5644. (b) Ma, C.; Zhang, J.; Li, F.; Zhang, R. *Eur. J. Inorg. Chem.* **2004**, 2775. (c) Ma, C.; Jiang, Q.; Zhang, R.; Wang, D. *Dalton Trans.* **2003**, 2975. (d) Ma, C.; Jiang, Q.; Zhang, R.; Wang, D. *Chem.–Eur. J.* **2006**, *12*, 420. (e) Jung, O.-S.; Sohn, Y. S.; Ibers, J. A. *Inorg. Chem.* **1986**, *25*, 2273. (f) Holeček, J.; Lyčka, A.; Nádvořník, M.; Handlřík, K. *Collect. Czech. Chem. Commun.* **1990**, *55*, 1193.

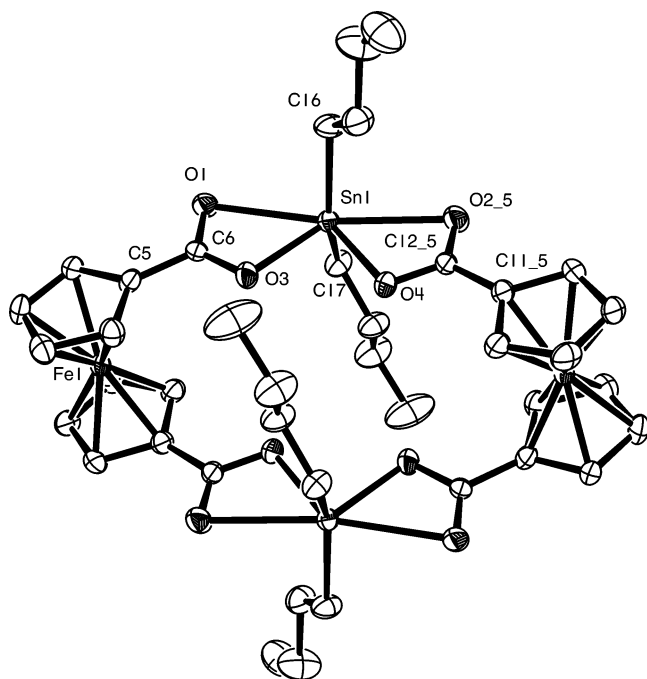


Figure 1. ORTEP diagram of **2** shown at 30% ellipsoidal probability level. Solvent molecules and hydrogen atoms have been omitted for the sake of clarity.

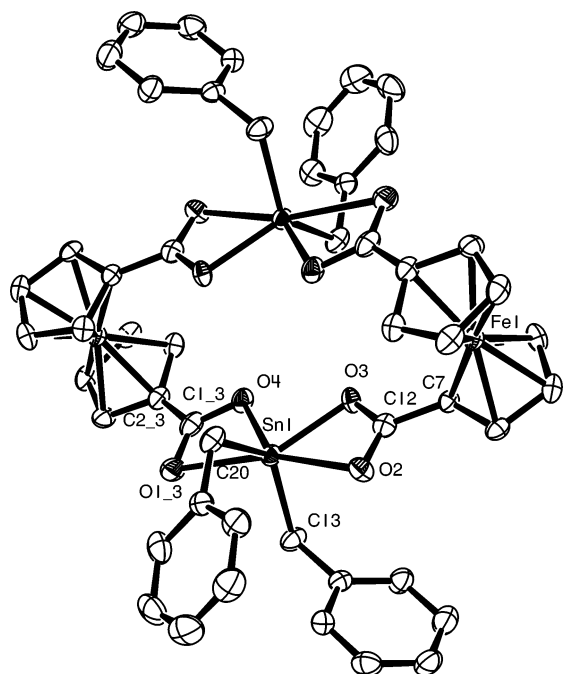


Figure 2. ORTEP diagram of **3** shown at 30% ellipsoidal probability level. Solvent molecules and hydrogen atoms have been omitted for the sake of clarity.

carboxylate ligands (see below). However, in solution, of the two coordinating carboxylate groups, if one is monodentate, five-coordination is achieved around tin (structure B, Chart 1). The proton NMR spectrum of **2** is consistent with this suggestion. Accordingly, four distinct cyclopentadienyl resonances are seen for **2** (see Experimental Section; Chart 1, structure B). In contrast **3** and **4** show only two cyclopentadienyl resonances in their proton NMR (see Experimental Section), suggesting that their solid-state structures are retained in solution also (Chart 1, structures A and C).

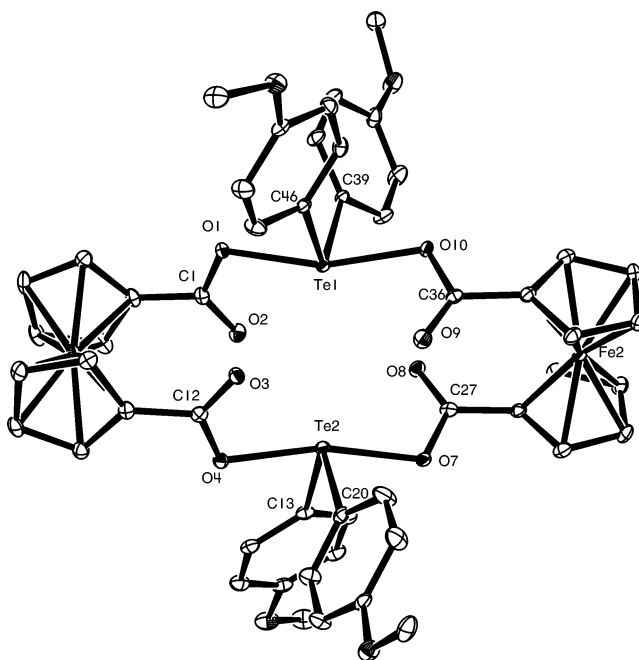


Figure 3. ORTEP diagram of **4** shown at 30% ellipsoidal probability level. Solvent molecules and hydrogen atoms have been omitted for the sake of clarity.

The IR spectra of **2–4** in the solid state show strong peaks at 1559 cm^{-1} (**2**), 1571 cm^{-1} (**3**), and 1617 and 1585 cm^{-1} (**4**). These are attributable to the $\nu_{\text{asym}}(\text{COO})$ stretch. The corresponding $\nu_{\text{sym}}(\text{COO})$ stretch is found at 1382 cm^{-1} (**2**), 1379 cm^{-1} (**3**), and 1396 and 1375 cm^{-1} (**4**). These values may be compared to those observed for LH_2 , 1675 [$\nu_{\text{asym}}(\text{COO})$] and 1300 cm^{-1} [$\nu_{\text{sym}}(\text{COO})$].^{7b} In general, $\nu_{\text{asym}}(\text{COO})$ for esters are lower than for free carboxylic acids; correspondingly the $\nu_{\text{sym}}(\text{COO})$ for esters moves up in comparison to carboxylic acids.^{4e} A similar trend is observed for metal carboxylates also.^{7b} The difference, Δ , [$\nu_{\text{asym}}(\text{COO}) - \nu_{\text{sym}}(\text{COO})$], of the asymmetric and symmetric carboxylate stretching frequencies can be indicative of anisobidentate chelating versus monodentate coordination of the carboxylate ligand. In the former the Δ values are smaller than in the latter.^{4e} In the present instance the Δ values for **2** and **3** are 177 and 192 cm^{-1} , while for **4** it is 221 cm^{-1} . This suggests that in **4** the carboxylate ligand binds in a monodentate manner to the metal ion, while in **2** and **3** it is bound in a chelating manner. These proposals are verified in the X-ray crystal structures of **2–4** (*vide infra*).

The UV–visible spectra of **2–4** show a broad band in the visible region at 453 (**2**), 454 (**3**), and 451 (**4**) nm, respectively. This band position is similar to what we had observed earlier in ferrocene-containing cyclophosphazenes^{2d} and is assigned to a d–d transition on the basis of earlier work by Gray and co-workers.¹⁰

Thermal analysis of **2–4** was studied by TGA and DSC (Figures S5–S7). Compound **2** shows a gradual weight loss until $\sim 120\text{ }^\circ\text{C}$ ($\sim 13\%$, attributable to the loss of two butyl groups). At this temperature a 9% weight loss occurs in a single sharp step. This corresponds to the loss of two molecules of CO_2 presumably from the carboxylate ligands. A sharp endotherm at $119\text{ }^\circ\text{C}$ corresponding to the onset of this process is seen in the DSC trace. Further gradual weight losses followed by an eventual sharp weight loss at $300\text{ }^\circ\text{C}$ are the features of the TGA of **2**. The TGA of **3** is marked by a gradual weight

(10) Sohn, Y. S.; Hendrickson, D. A.; Gray, H. B. *J. Am. Chem. Soc.* **1971**, *93*, 3603.

Table 1. Selected Bond Distance and Bond Angle Data for 2 and 3

compound 2				compound 3			
bond distances (Å)		bond angles (deg)		bond distances (Å)		bond angles (deg)	
Sn(1)–O(3)	2.111(4)	O(3)–Sn(1)–O(4)	82.04(13)	Sn(1)–O(4)	2.093(4)	O(4)–Sn(1)–O(3)	84.90(15)
Sn(1)–O(4)	2.114(3)	O(3)–Sn(1)–C(17)	103.3(2)	Sn(1)–O(3)	2.093(4)	O(4)–Sn(1)–C(13)	103.0(2)
Sn(1)–C(17)	2.114(6)	O(4)–Sn(1)–C(17)	105.08(18)	Sn(1)–C(13)	2.128(6)	O(3)–Sn(1)–C(13)	107.0(2)
Sn(1)–C(16)	2.115(6)	C(17)–Sn(1)–C(16)	142.08(22)	Sn(1)–C(20)	2.137(6)	O(4)–Sn(1)–C(20)	110.57(19)
Sn(1)–O(1)	2.592(4)	O(3)–Sn(1)–C(16)	105.43(20)	Sn(1)–O(2)	2.481(4)	O(3)–Sn(1)–C(20)	113.4(2)
Sn(1)–O(2_5)	2.561(4)	O(4)–Sn(1)–C(16)	102.96(19)	Sn(1)–O(1_3)	2.536(4)	C(13)–Sn(1)–C(20)	128.8(3)
O(1)–C(6)	1.239(6)	O(1)–Sn(1)–O(4)	136.80 (14)	O(1_3)–C(1_3)	1.239(7)	O(4)–Sn(1)–O(2)	141.49(15)
O(2_5)–C(12_5)	1.250(6)	O(2_5)–Sn(1)–O(3)	137.21(15)	O(2)–C(12)	1.248(7)	O(3)–Sn(1)–O(2)	56.61(13)
O(3)–C(6)	1.297(6)	O(2_5)–Sn(1)–C(17)	89.40(20)	O(3)–C(12)	1.302(6)	C(13)–Sn(1)–O(2)	90.66(18)
O(4)–C(12_5)	1.283(6)	O(2_5)–Sn(1)–C(16)	86.09(20)	O(4)–C(1_3)	1.291(7)	C(20)–Sn(1)–O(2)	86.4(2)
		O(2_5)–Sn(1)–O(4)	55.17 (14)			O(4)–Sn(1)–O(1_3)	55.24(14)
		O(1)–Sn(1)–O(2_5)	167.99 (13)			O(3)–Sn(1)–O(1_3)	140.01(14)
						C(13)–Sn(1)–O(1_3)	81.82(19)
						C(20)–Sn(1)–O(1_3)	86.7(2)
						O(2)–Sn(1)–O(1_3)	163.22(13)

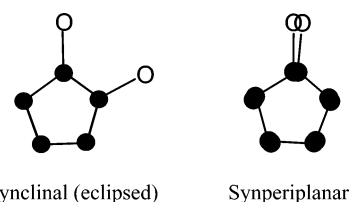
Table 2. Important Bond Distance and Bond Angle Data for 4

bond distances (Å)		bond angles (deg)	
Te(1)–C(46)	2.096(4)	C(20)–Te(2)–C(13)	99.36(15)
Te(1)–C(39)	2.100(4)	C(20)–Te(2)–O(7)	82.27(12)
Te(1)–O(1)	2.145(2)	C(13)–Te(2)–O(7)	89.14(13)
Te(1)–O(9)	2.978(3)	C(20)–Te(2)–O(4)	86.41(12)
Te(1)–O(2)	2.909(3)	C(13)–Te(2)–O(4)	84.72(13)
Te(2)–O(3)	2.911(2)	O(7)–Te(2)–O(4)	166.09(9)
Te(2)–O(8)	3.015(3)	C(46)–Te(1)–C(39)	102.28(14)
Te(1)–O(10)	2.167(3)	C(46)–Te(1)–O(1)	83.11(12)
Te(2)–C(20)	2.108(4)	C(39)–Te(1)–O(1)	87.93(12)
Te(2)–C(13)	2.117(4)	C(46)–Te(1)–O(10)	87.91(12)
Te(2)–O(7)	2.144(3)	C(39)–Te(1)–O(10)	79.67(12)
Te(2)–O(4)	2.155(3)	O(1)–Te(1)–O(10)	162.80(10)
O(10)–C(36)	1.315(4)		
O(11)–C(42)	1.364(5)		
O(11)–C(43)	1.425(5)		
O(12)–C(49)	1.357(4)		
O(1)–C(1)	1.319(5)		
O(2)–C(1)	1.228(5)		
O(3)–C(12)	1.226(5)		
O(4)–C(12)	1.317(4)		
O(5)–C(16)	1.363(5)		
O(5)–C(17)	1.420(5)		
O(6)–C(23)	1.368(4)		
O(6)–C(26)	1.433(5)		
O(7)–C(27)	1.331(4)		
O(8)–C(27)	1.220(4)		
O(9)–C(36)	1.226(4)		
O(12)–C(50)	1.443(5)		

loss (22%) until ~250 °C. At this point the weight loss is more sudden and is nearly complete at ~420 °C. The TGA trace of **4** is different from that of **2** and **3**. This compound is thermally more stable than the corresponding tin analogues. There is virtually no weight loss until 230 °C. At this stage there is a precipitous weight loss of about 52% (loss of the substituents on tellurium and the carboxylate groups on ferrocene) followed by a further gradual weight loss. The final char residue for this compound is ~14%.

X-ray Crystal Structures of 2–4. The ORTEP diagrams of **2–4** are given in Figures 1–3. The important bond distance/angle parameters for these compounds are summarized in Tables 1 and 2.

The molecular structures of **2** and **3** are similar and show the presence of a 16-membered heterobimetallic tetranuclear macrocyclic ring. Each macrocycle contains alternately two tin centers, which are bridged to each other by the coordination of two ferrocenedicarboxylate ligands. Each ferrocenedicarboxylate ligand binds to two different tin atoms in an anisobidentate chelating coordination mode characterized by the presence of two types of Sn–O bond distances: one short Sn–O distance

Chart 2. Conformations of the Ferrocenedicarboxylate Ligands in 2–4^a

^a Synclinal (eclipsed) conformation corresponds to the situation where the two cyclopentadienyl groups are perfectly eclipsed while the 1,1' substituents on these rings are not. In synperiplanar conformation the two cyclopentadienyl rings are perfectly eclipsed; the two substituents on the 1,1' positions are also nearly eclipsed, with a small torsion angle.

[av 2.113(4) Å (**2**) and av 2.093 (4) Å (**3**)] and one long Sn–O distance [av 2.577(4) Å (**2**) and av 2.509 (4) Å (**3**)]. These data may be compared with that found in *n*-Bu₂Sn[O₂CFC]₂ (Sn–O, av 2.122(3) and av 2.542(4) Å).^{2b} The tin atom present in the latter possesses a coordination environment that is similar to that found in **2** and **3**. The long Sn–O distance found in both **2** and **3** is, however, much shorter than the sum of the van der Waals radii of tin and oxygen (3.7 Å).¹¹ The anisobidentate chelating coordination mode of the ferrocenedicarboxylate ligands in **2** and **3** is reflected in the C–Oav bond distances also [1.245(6) and 1.290(6) Å (**2**); 1.244(7) and 1.297(7) Å (**3**)].

The coordination environment around tin in both **2** and **3** comprises of a 4O, 2C set. The coordination geometry around tin can be described as skewed trapezoidal bipyramid. The C–Sn–C angles in **2** and **3** are 142.1(2)° and 128.8 (3)°, respectively. Of the O–Sn–O angles, one is much wider than the others. For example, in **2**, the O1–Sn1–O2_5 angle is 167.99(1)°, while O3–Sn1–O4 is 82.04(1)°.

The two ferrocenedicarboxylate groups in **2** and **3** are nearly parallel to each other (Figures 1 and 2). The overall conformation of the ferrocenedicarboxylate group can be described as synclinal (eclipsed) with torsion angles of 63.7° and 61.0°, respectively for **2** and **3** (Chart 2). This conformation descriptor is based on the definitions used in [1,1']-ferrocenophanes¹² and implies that the two cyclopentadienyl groups of the ferrocene-

(11) (a) Ma, C.; Han, Y.; Zhang, R.; Wang, D. *Dalton Trans.* **2004**, 1832. (b) Casas, J. S.; Castineiros, A.; Martinez, E. G.; Gonzales, A. S.; Sanches, A.; Sordo, J. *Polyhedron* **1997**, *16*, 795.

(12) (a) Löwendahl, J. M.; Håkansson, M. *Organometallics* **1995**, *14*, 4736. (b) Mueller-Westerhoff, U. T.; Swiegers, G. F.; Haas, T. J. *Organometallics* **1992**, *11*, 3411. (c) Mai, J. F.; Yamamoto, Y. J. *Organomet. Chem.* **1998**, *560*, 223.

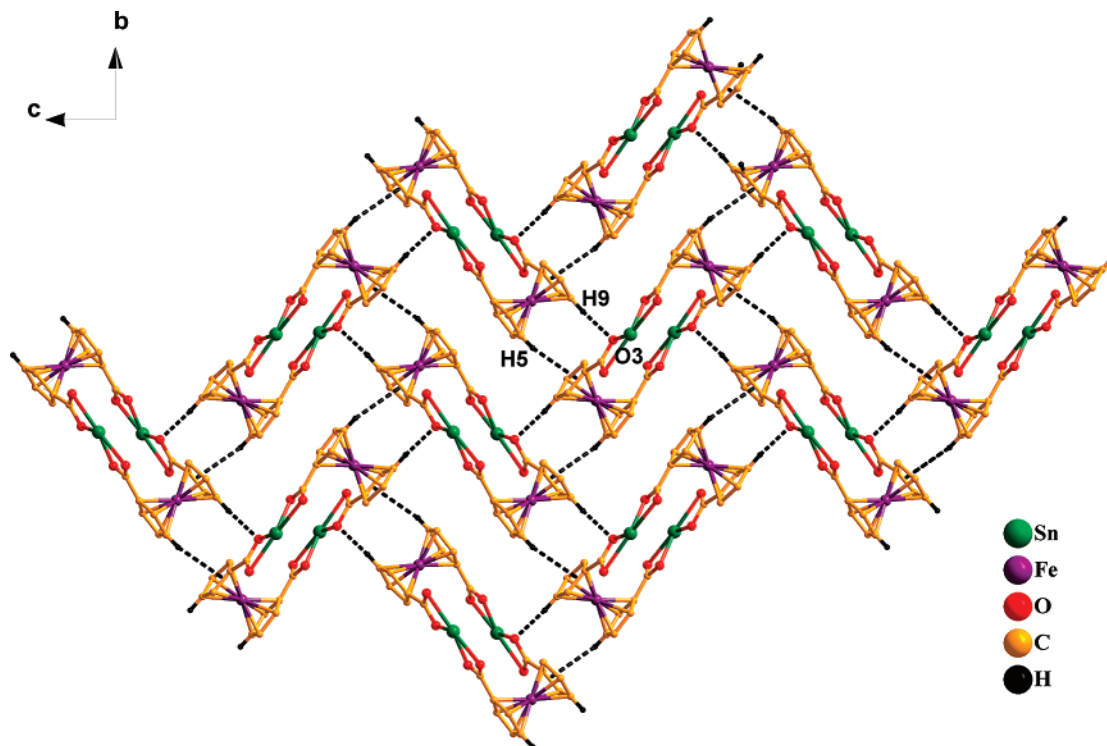


Figure 4. 2D-Supramolecular network of **3** showing interconnected zigzag polymers. The secondary interactions involved in the formation of this supramolecular architecture are $C-H_{(\text{ferrocene})} \cdots \pi$ and $C-H \cdots O$ interactions. Benzyl groups and hydrogen atoms have been removed for the sake of clarity. The metric parameters involved are as follows: $C5-H5$ 0.980 Å, $C5-H5 \cdots \pi$ 3.146 Å, $C5-H5 \cdots \pi$ 122.938°, $C9-H9$ 0.979 Å, $H9-O3$ 2.447 Å, and $C9-H9-O3$ 164.420°. Symmetry operators: $x, 1.5-y, 0.5+z$ and $-x, 0.5+y, 0.5-z$.

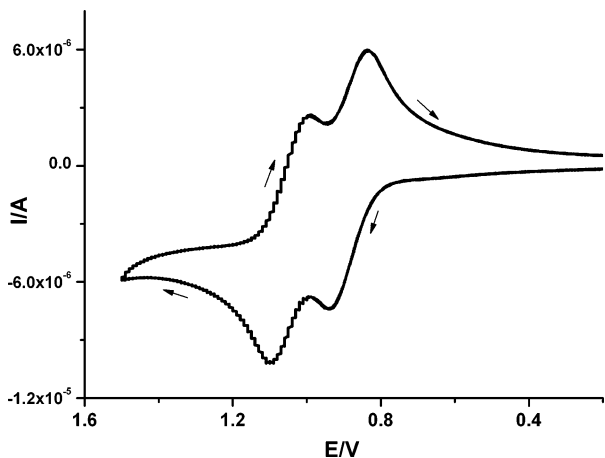


Figure 5. Cyclic voltammogram of **2**.

dicarboxylate ligand perfectly eclipse each other. On the other hand, the two carboxylate substituents present on 1,1' positions do not eclipse each other. The four metal centers present in **2** and **3** are coplanar (Figure S8) and occupy the corners of a distorted rhombus whose sides measure 5.469(2) and 5.707(1) Å for **2** and 5.4024(9) and 5.518(1) Å for **3**.

The molecular structure of the organotellurium macrocycle **4** is grossly similar to that of its tin analogues **2** and **3** (Figure 3). Two important differences are present, however. First, the ferrocene carboxylate ligand can be considered as monodentate. The short Te–O distance involved [av 2.153 (4) Å] is much shorter than the longer Te–O bond (av 2.953 (3) Å). Although, the latter is still shorter than the sum of the van der Waals radii of tellurium and oxygen (3.6 Å),¹³ we are hesitant to view this

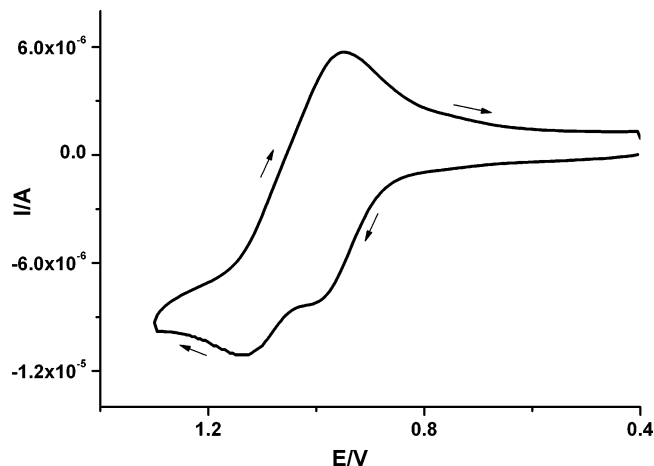


Figure 6. Cyclic voltammogram of **3**.

Table 3. Electrochemical Data for Compounds 2–4^a

compound	$E_{1/2}, V$	$(\Delta E_p, mV)^b$	K_c^c	ref
2	0.89(100)	1.05(110)	5.07×10^2	this work
3	0.98(60)	1.14 ^d		this work
4	0.77(80)	0.88(70)	0.72×10^2	this work
$[n\text{-BuSn}(\text{O})\text{OC}(\text{O})\text{Fc}]_6$	0.77(128)			2a
$[n\text{-BuSn}(\text{O})\text{OC}(\text{O})\text{CH}_2\text{Fc}]_6$	0.55(240)			2c
$[n\text{-Bu}_2\text{Sn}[\text{OC}(\text{O})\text{Fc}]_2]$	0.75(158)			2b

^a Measured in CH_2Cl_2 containing $[n\text{-Bu}_4\text{N}][\text{PF}_6]$ at a scan rate of 100 mV s^{-1} . The peak potentials are with respect to Ag/AgCl . ^b $E_{1/2} = (E_{pc} + E_{pa})/2$. ^c $K_c = 10^{\Delta E/59.15 \text{ mV}}$ at 298 K. ^d Irreversible process.

as a coordination interaction. Consequently, the coordination number around tellurium may be described as four (2C, 2O) with the tellurium atom being present in a *seesaw* geometry. The latter is consistent with the presence of a stereochemically active lone pair on tellurium. Another difference between the structural features of **4** and that of **2** and **3** is that the two

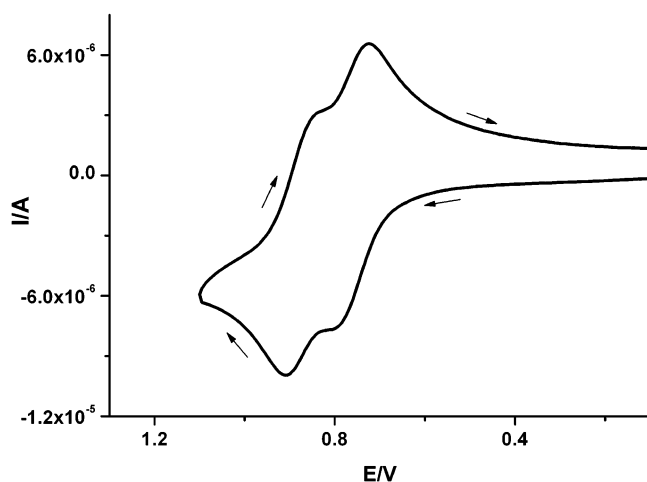
(13) Kobayashi, K.; Izawa, H.; Yamaguchi, K.; Horn, E.; Furukawa, N. *Chem. Commun.* **2001**, 1428.

Table 4. Crystallographic Data for Compounds 2–4

	2	3	4
empirical formula	C ₁₇₈ H ₂₂₆ Fe ₈ O ₃₂ Sn ₈	C ₅₄ H ₄₈ Cl ₄ Fe ₂ O ₈ Sn ₂	C ₅₃ H ₄₆ Cl ₂ Fe ₂ O ₁₂ Te ₂
fw	4273.91	1315.80	1312.70
temp (K)	273(2)	273(2)	273(2)
wavelength (Å)	0.71073	0.71073	0.71073
cryst syst	monoclinic	monoclinic	monoclinic
space group	C2/c	P2(1)/c	P2(1)/n
unit cell dimens			
<i>a</i> (Å), α (deg)	25.500(5), 90	13.5963(16), 90	15.2410(7), 90
<i>b</i> (Å), β (deg)	9.7417(19), 115.42(3)	10.3361(12), 105.662(2)	21.6111(11), 103.56(10)
<i>c</i> (Å), γ (deg)	19.954(4), 90	19.075(2), 90	15.7105(8), 90
volume (Å ³), <i>Z</i>	4477.1(15), 1	2581.1(15), 2	5030.4(4), 4
ρ _{calcd} (g cm ⁻³)	1.585	1.693	1.733
absorp coeff (mm ⁻¹)	1.787	1.768	1.883
<i>F</i> (000)	2158	1312	2600
cryst size (mm)	0.2 × 0.3 × 0.2	0.3 × 0.2 × 0.2	0.3 × 0.3 × 0.2
θ range for data collection (deg)	2.19 to 26.50	2.26 to 27.00	1.92 to 25.00
limiting indices	-28 ≤ <i>h</i> ≤ 32, -12 ≤ <i>k</i> ≤ 12, -25 ≤ <i>l</i> ≤ 16	-17 ≤ <i>h</i> ≤ 17, -9 ≤ <i>k</i> ≤ 13, -23 ≤ <i>l</i> ≤ 24	-18 ≤ <i>h</i> ≤ 17, -25 ≤ <i>k</i> ≤ 18, 17, -18 ≤ <i>l</i> ≤ 18
no. of reflns collected	12 750	15 379	25 955
no. of indep reflns	4626	5586	8863
	[<i>R</i> (int) = 0.0601]	[<i>R</i> (int) = 0.0694]	[<i>R</i> (int) = 0.0374]
no. of obsd reflns	3313	3371	7515
absorp corr	empirical	empirical	empirical
no. of data/restraints/params	4626/0/249	5586/0/316	8863/0/645
goodness-of-fit on <i>F</i> ²	0.972	1.008	1.034
final <i>R</i> indices [<i>I</i> > 2σ(<i>I</i>)]	<i>R</i> 1 = 0.0515, w <i>R</i> 2 = 0.1171	<i>R</i> 1 = 0.0528, w <i>R</i> 2 = 0.0941	<i>R</i> 1 = 0.0357, w <i>R</i> 2 = 0.0772
<i>R</i> indices (all data)	<i>R</i> 1 = 0.0773, w <i>R</i> 2 = 0.1290	<i>R</i> 1 = 0.1016, w <i>R</i> 2 = 0.1173	<i>R</i> 1 = 0.0452, w <i>R</i> 2 = 0.0811
largest diff peak and hole (e Å ⁻³)	0.864 and -0.519	0.901 and -0.617	1.107 and -1.084

ferrocene ligands in **4** are nearly orthogonal to each other (88.2°). The conformation of the ferrocenecarboxylate ligand in **4** is synperiplanar, with torsion angles of 2.1° and 12.2° (Chart 2).

We have reported earlier that organostannoxane-supported multiferrrocene assemblies show a very rich supramolecular organization in their solid state owing to multiple intermolecular interactions, chief among them being C–H...O interactions involving the acidic C–H's of the ferrocene groups and the oxygen atoms of the carboxylate moieties.^{2b,c} In the present instance also a very rich supramolecular organization is seen in their solid-state structures (Figures S9–S15). As a representative example, the supramolecular organization observed in **3** is described. In this case the ferrocene moieties of alternate molecules are involved in a C–H...π (T-shaped; end-face) and C–H...O interactions. This results in the formation of a two-dimensional network containing interconnected zigzag

**Figure 7.** Cyclic voltammogram of **4**.

polymer chains (Figure 4). Further interactions involving the C–H moiety of the benzyl substituent and the aromatic unit of the benzyl group leads to a three-dimensional network (Figure S11).

Electrochemical Studies. Cyclic voltammetric studies were carried out on **2–4** (Figures 5–7). The data for these compounds along with literature data on some related compounds are given in Table 3. Previous electrochemical studies on organostannoxane-supported assemblies such as [*n*-BuSn(O)O₂CFc]₆,^{2a} [*n*-BuSn(O)O₂CCH₂Fc]₆,^{2c} and [*n*-Bu₂Sn{OC(O)Fc}₂]₂^{2b} showed a single quasi-reversible oxidation. Although the nature of the organostannoxane core varied in these compounds, the oxidation peak potential of the ferrocene periphery remained virtually invariant (Table 3). This suggested a complete absence of electronic communication between the various individual ferrocene units present in these assemblies. In contrast, in the current study we have observed that **2** and **4** showed two quasi-reversible single-electron oxidations. The *E*_{1/2} values for these processes are 0.89 and 1.05 V (**2**) and 0.77 and 0.88 V (**4**) (Figures 5 and 7). We have carried out continuous cyclic voltammetric studies five times and did not observe any change in peak potential. In contrast, **3** shows a quasi-reversible *E*_{1/2} process at 0.98 V and an irreversible one at 1.14 V (Figure 6). The extent of electronic communication between the two ferrocene units in **2** and **4** can be assessed by examining their comproportionation constants (*K*_c). On the basis of this value, following the Robin–Day classification,¹⁴ compounds **2** and **4** can be classified as belonging to an intermediate class between class I (noncoupling) and class II (weakly coupled) systems.

Conclusions

The reaction between the difunctional reagents 1,1'-ferrocenedicarboxylic acid and diorganotin or -tellurium dichlorides

(14) (a) Robin, M. B.; Day, P. *Adv. Inorg. Chem. Radiochem.* **1967**, *10*, 247. (b) Kaim, W.; Klein, A.; Glöckle, M. *Acc. Chem. Res.* **2000**, *33*, 755.

affords, cleanly, in near quantitative yields, lipophilic 16-membered heterobimetallic tetranuclear macrocyclic ring systems. Unlike previously studied organostannoxane-supported multi-ferrocene compounds, the macrocyclic compounds prepared in the current study show an electronic communication between the two ferrocene units. This raises the possibility that the strength of such electronic communication between multiple redox units can be modulated by changing the nature of the cluster/cage/ring that supports such redox units. Also, the nature of the redox-active ligand as well as its binding mode with the bridging/supporting/connecting redox-inactive motif would appear to be important in determining the eventual redox properties of such assemblies. We are currently engaged in unraveling these features.

Experimental Section

General Remarks. All the reactions were carried out under a dry atmosphere using standard Schlenck techniques. Solvents were dried prior to use. Dibenzyltin dichloride and bis(4-methoxyphenyl)-tellurium dichloride were prepared by previously reported procedures.¹⁵ Dibutyltin dichloride (Fluka) and 1,1'-ferrocenedicarboxylic acid (Aldrich) were used as received without further purification. Melting points were measured using a JSGW melting point apparatus and are uncorrected. IR spectra were recorded from 4000 to 400 cm⁻¹ on a Bruker FT-IR Vector 22 model in the solid state using KBr pellets. UV-visible spectra were recorded on a Perkin-Elmer LS UV-vis Lambda 20 spectrometer using CH₂Cl₂ as the solvent. Elemental analyses were performed using a Thermoquest CE Instruments model EA/110 CHNS-O elemental analyzer. ¹H and ¹¹⁹Sn{¹H} NMR spectra were obtained on a JEOL-JNM Lambda model 400 spectrometer using CDCl₃ solutions with the corresponding chemical shifts referenced to tetramethylsilane and tetramethyltin, respectively. Cyclic voltammetric studies were performed on a BAS Epsilon electrochemical workstation in CH₂-Cl₂ with 0.1 M [*n*-Bu₄N][PF₆] as the supporting electrolyte. The working electrode was a BAS Pt disk electrode, the reference electrode was Ag/AgCl, and the auxiliary electrode was a Pt wire. The ferrocene/ferrocenium couple occurs at $E_{1/2} = +0.51$ (70) V versus Ag/AgCl under the same experimental conditions. ESI-MS spectra were recorded on a Micromass Quattro II triple quadrupole mass spectrometer. TGA and DSC curves were obtained on a Perkin-Elmer, Pyris6 thermogravimetric analyzer at a heating rate of 10 °C/min under argon.

Synthesis. A general synthetic procedure has been utilized for the preparation of the macrocycles **2–4**. A detailed procedure is given below for the preparation of **2**.

[[*n*-Bu)₂Sn(L)]₂ (2**).** In 25 mL of benzene, 1,1'-ferrocenedicarboxylic acid, LH₂ (**1**) (0.13 g, 0.47 mmol), and triethylamine (0.11 g, 1.00 mmol) were added and stirred for 5 min. Immediately afterward dibutyltin dichloride (0.14 g, 0.46 mmol) was added, and the reaction mixture was heated under reflux for 6 h. It was allowed to cool to room temperature and filtered to separate a crystalline product formed in the reaction. The latter was washed with 30 mL of acetonitrile/water (1:1) to remove triethylammonium hydrochloride. The residue was recrystallized from tetrahydrofuran/*n*-hexane (1:1) at room temperature by a slow diffusion method. Yield: 0.22 g (95%). UV-visible (CH₂Cl₂) λ_{\max}/nm ($\epsilon/\text{dm}^3 \text{ mol}^{-1} \text{ cm}^{-1}$): 453 (559). Mp: >300 °C (dec). Anal. Calcd for C₄₀H₅₂O₈Sn₂Fe₂: C, 47.57; H, 5.19. Found: C, 47.31; H, 5.10. IR (KBr, cm⁻¹): 1559 [s, $\nu_{\text{asym}}(\text{COO})$] and 1382 [s, $\nu_{\text{sym}}(\text{COO})$]. ¹H NMR (400 MHz, CDCl₃, ppm): δ 4.89 (s, 1H, ferrocenyl), 4.68 (s, 1H, ferrocenyl),

4.61 (s, 1H, ferrocenyl), 4.40 (s, 1H, ferrocenyl), 0.87–1.68 (m, 9H, butyl). ¹¹⁹Sn NMR (150 MHz, ppm): δ -152.2 (s). ESI-MS: m/z (%) 1011.05 [(*n*-Bu)₂Sn(L)]₂ + H]⁺ (17), 507.03 [(*n*-Bu)₂Sn(L)] + H]⁺ (100).

[(Bn)₂Sn(L)]₂ (3**).** The quantities involved are **1** (0.06 g, 0.22 mmol), triethylamine (0.05 g, 0.50 mmol), and dibenzyltin dichloride (0.08 g, 0.22 mmol). The solid residue (after removal of triethylammonium hydrochloride by acetonitrile/water wash) was recrystallized from dichloromethane by a slow evaporation method at room temperature. Yield: 0.1 g (81%). UV-visible (CH₂Cl₂) λ_{\max}/nm ($\epsilon/\text{dm}^3 \text{ mol}^{-1} \text{ cm}^{-1}$): 454 (623). Mp: >300 °C dec. Anal. Calcd for C₅₂H₄₄O₈Sn₂Fe₂: C, 54.50; H, 3.87. Found: C, 54.62; H, 3.83. IR (KBr, cm⁻¹): 1571 [s, $\nu_{\text{asym}}(\text{COO})$] and 1379 [s, $\nu_{\text{sym}}(\text{COO})$]. ¹H NMR (400 MHz, CDCl₃, ppm): δ 7.09 (s, br, 20H, aromatic), 4.95 (s, br, 8H, ferrocenyl), 4.45 (s, br, 8H, ferrocenyl), 2.94 (s, br, 8H, Ar-CH₂). ¹¹⁹Sn NMR (150 MHz, ppm): δ -259.2 (s). ESI-MS: m/z (%) 1146.99 [(Bn)₂Sn(L)]₂ + H]⁺ (24), 575.00 [(Bn)₂Sn(L)] + H]⁺ (58).

[(*p*-MeOC₆H₄)₂Te(L)]₂ (4**).** The quantities involved are **1** (0.05 g, 0.18 mmol), triethylamine (0.04 g, 0.40 mmol), and bis(4-methoxyphenyl)tellurium dichloride (0.08 g, 0.19 mmol). In this case the reaction mixture was allowed to stir at room temperature for 24 h. The residue obtained (after removing triethylammonium hydrochloride by acetonitrile/water wash) was recrystallized from a mixture of dichloromethane/*n*-hexane by a slow diffusion method at 0 °C. Yield: 0.11 g (93%). UV-visible (CH₂Cl₂) λ_{\max}/nm ($\epsilon/\text{dm}^3 \text{ mol}^{-1} \text{ cm}^{-1}$): 451 (397). Mp: >300 °C dec. Anal. Calcd for C₅₂H₄₄O₁₂Te₂Fe₂: C, 50.87; H, 3.61. Found: C, 50.25; H, 3.80. IR (KBr, cm⁻¹): 1617, 1585 [s, $\nu_{\text{asym}}(\text{COO})$] and 1396, 1375 [s, $\nu_{\text{sym}}(\text{COO})$]. ¹H NMR (400 MHz, CDCl₃, ppm): δ 8.05 (d, $J = 8.8$ Hz, 4H, aromatic), 6.99 (d, $J = 9.0$ Hz, 4H, aromatic), 4.90 (s, 4H, ferrocenyl), 4.31 (s, 4H, ferrocenyl), 3.83 (s, 6H, methoxy). MS: m/z (%) 1228.97 [(Ar)₂Te(L)]₂ + H]⁺ (50), 614.99 [(Ar)₂Te(L)] + H]⁺ (100).

X-ray Crystallographic Study. Single crystals of **2** were obtained by vapor diffusion of *n*-hexane into a solution of **2** in tetrahydrofuran. It is to be noted that the structure of **2** showed the presence of benzene molecules in the unit cell. The source of this may be traced to the fact that benzene was used as the solvent for the preparation of **2**. Crystals of **3** were obtained by slow evaporation of its solution in CH₂Cl₂. Single crystals of **4** were obtained by vapor diffusion of *n*-hexane into its solution in CH₂-Cl₂ in a refrigerator at 0 °C. Suitable crystals for single-crystal X-ray diffraction measurements were mounted on a CCD Bruker SMART APEX diffractometer. Data were collected at 273(2) K using graphite-monochromated Mo K α radiation ($\lambda_{\alpha} = 0.71073$ Å). The structures were solved by direct methods and refined (SHELXL 97)¹⁶ by full matrix least-squares procedures on F^2 . The hydrogen atoms were included in idealized positions and were refined according to the riding model. Non-hydrogen atoms were refined with anisotropic displacement parameters, with the exception of the benzene (solvent) molecule in **2** and the CH₂Cl₂ molecule in **4**. In **2**, all the carbon atoms of the solvent molecule (benzene) were disordered with 75% occupancy, and in **4** the CH₂Cl₂ molecules were disordered and were modeled satisfactorily with a 50:50 site occupancy.

Acknowledgment. We are thankful to the Department of Science and Technology, New Delhi, for financial support. R.T. thanks the Council of Scientific and Industrial Research, India, for a Senior Research Fellowship. V.C. is the Lalit Kapoor Professor of Chemistry at Indian Institute of Technology, Kanpur. V.C. is thankful to the Department of Science and

(15) (a) Sisido, K.; Takeda, Y.; Kinugawa, Z. *J. Am. Chem. Soc.* **1961**, *83*, 538. (b) Jolly, W. L. *The Synthesis and Characterization of Inorganic Compounds*, Prentice Hall: Engle-Wood Cliffs, NJ, 1970. (c) Bergman, J. *Tetrahedron* **1972**, *28*, 3323.

(16) (a) Sheldrick, G. M. *SHELXL-97*, Program for Crystal Structure Refinement; University of Göttingen: Göttingen, Germany, 1997. (b) Sheldrick, G. M. *SHELXTL*, Reference Manual: Version 5.1; Bruker AXS: Madison, WI, 1998.

Technology for a J. C. Bose National Fellowship. We thank Dr. J. K. Bera and A. Sinha, Department of Chemistry, Indian Institute of Technology, Kanpur, for their help with electrochemical studies. We thank Dr. S. P. Rath, Department of Chemistry, Indian Institute of Technology, Kanpur, for his help with X-ray crystallography.

Supporting Information Available: Crystallographic information files (CIF) for compounds **2–4** and Figures S1–S15. This material is available free of charge via the Internet at <http://pubs.acs.org>.

OM700622R